BIOLOGY OF REPRODUCTION **80,** 124–133 (2009)
Published online before print 17 September 2008.
DOI 10.1095/biolreprod.108.068882

Sorbitol Can Fuel Mouse Sperm Motility and Protein Tyrosine Phosphorylation via Sorbitol Dehydrogenase[1]

Wenlei Cao,[3] Haig K. Aghajanian,[3] Lisa A. Haig-Ladewig,[3] and George L. Gerton[2,3,4]

Center for Research on Reproduction and Women's Health,[3] Department of Obstetrics and Gynecology,[4] University of Pennsylvania School of Medicine, Philadelphia, Pennsylvania 19104

ABSTRACT

Energy sources that can be metabolized to yield ATP are essential for normal sperm functions such as motility. Two major monosaccharides, sorbitol and fructose, are present in semen. Furthermore, sorbitol dehydrogenase (SORD) can convert sorbitol to fructose, which can then be metabolized via the glycolytic pathway in sperm to make ATP. Here we characterize *Sord* mRNA and SORD expression during mouse spermatogenesis and examine the ability of sorbitol to support epididymal sperm motility and tyrosine phosphorylation. *Sord* mRNA levels increased during the course of spermatogenic differentiation. SORD protein, however, was first detected at the condensing spermatid stage. By indirect immunofluorescence, SORD was present along the length of the flagella of caudal epididymal sperm. Furthermore, immunoelectron microscopy showed that SORD was associated with mitochondria and the plasma membranes of sperm. Sperm incubated with sorbitol maintained motility, indicating that sorbitol was utilized as an energy source. Sorbitol, as well as glucose and fructose, were not essential to induce hyperactive motility. Protein tyrosine phosphorylation increased in a similar manner when sorbitol was substituted for glucose in the incubation medium used for sperm capacitation. These results indicate that sorbitol can serve as an alternative energy source for sperm motility and protein tyrosine phosphorylation.

epididymis, flagellum, sorbitol, sorbitol dehydrogenase, sperm, spermatogenesis, sperm capacitation, sperm motility and transport

INTRODUCTION

Unlike most mammalian cells, sperm are highly motile and consume considerable amounts of energy. Furthermore, sperm spend a substantial amount of time maturing in the male and female reproductive tracts before they become competent for fertilization. As a consequence, sperm must maintain the ability to produce and utilize energy efficiently. Although sperm of some species have been reported to utilize glycogen to survive longer in vivo [1], the consensus is that sperm rely heavily on energy sources from the extracellular milieu to support their energy needs. Mammalian sperm generally utilize monosaccharides for energy [2], from ubiquitous glucose to less-common sugars, such as fructose or sorbitol [2–5], as well as other carbon sources, such as lactate, pyruvate, citrate, and glycerol [5–7].

All tissues in the male reproductive tract, except the testis, have the ability to produce sorbitol and fructose [8]. Unlike other body fluids, fructose—instead of glucose—is generally the principal reducing sugar in seminal plasma, and thus serves as the main glycolyzable substrate for spermatozoa in semen [9]. Depending on the species, seminal plasma fructose concentrations vary from high levels in bull and ram to lower amounts in other species, such as dog and stallion, where it is essentially absent [10]. However, even in the semen of species where fructose is low, sorbitol is always present [10]. Sorbitol is also detected in the female reproductive tract [11, 12].

Sorbitol dehydrogenase (SORD), which oxidizes sorbitol to fructose at the expense of one molecule of NAD being converted to NADH, was first detected in sperm by enzymatic assays [13]. Until now, a limited number of investigations have been carried out on a variety of species, but most of these studies focus on the distribution of SORD in male accessory glands [8, 14–16]. Although sorbitol can be utilized by sperm, no study has focused on the detailed expression or localization of SORD in sperm, or on the ability of sorbitol to support sperm motility and capacitation. Here, we demonstrate the expression of *Sord* mRNA and protein in mouse spermatogenic cells and sperm, determine the subcellular localization of SORD during sperm maturation, and provide direct evidence of a role for sorbitol in sperm motility and tyrosine phosphorylation.

MATERIALS AND METHODS

Sperm and Germ Cell Preparation

All animal procedures were approved by the University of Pennsylvania Institutional Animal Care and Use Committee. Male germ cells were prepared from decapsulated testes of adult mice (CD1 retired breeders; Charles River Laboratories) by sequential dissociation with collagenase and trypsin-DNase I [17]. To purify populations of pachytene spermatocytes, round spermatids, and condensing spermatids, the cells were separated at unit gravity in a 2%–4% BSA gradient in enriched Krebs-bicarbonate medium [18]. Both the pachytene spermatocyte and round spermatid populations were at least 85% pure as determined by microscopic examination and differential counting with a hemocytometer, while the condensing spermatid population was approximately 40%–50% pure, with the balance primarily being anucleate residual bodies and round spermatids.

Epididymal sperm were collected by mincing the caudae epididymides and allowing the sperm to swim out in PBS (2.68 mM KCl, 136.09 mM NaCl, 1.47 mM KH_2PO_4, 8.07 mM Na_2HPO_4, pH 7.4). The supernatant containing sperm was gently aspirated, and sperm (>99% pure as assessed by light microscopy) were collected by centrifugation at $800 \times g$ for 5 min at room temperature. The sperm were then homogenized in 1% SDS, 75 mM NaCl, 24 mM EDTA, pH 6.0 (S-EDTA), layered onto a 1.6 M sucrose cushion in S-EDTA, and centrifuged at $5000 \times g$ for 1 h at room temperature. The SDS-resistant tail structures (sperm accessory structures) were collected from the interface [19]. The purity was visually checked by light microscopy (Supplemental Fig. S1 and all other supplemental data are available online at www.biolreprod.org). Previous results demonstrated the purity by electron microscopy and immunoblotting [20, 21].

[1]Supported by National Institute of Child Health and Human Development grant P01-HD006274 to G.L.G.
[2]Correspondence: George L. Gerton, Center for Research on Reproduction and Women's Health, Department of Obstetrics and Gynecology, University of Pennsylvania School of Medicine, 421 Curie Blvd., 1311 BRB II/III, Philadelphia, PA 19104-6160. FAX: 215 5737627; e-mail: gerton@mail.med.upenn.edu

Received: 4 March 2008.
First decision: 29 March 2008.
Accepted: 9 September 2008.

ISSN: 0006-3363. http://www.biolreprod.org

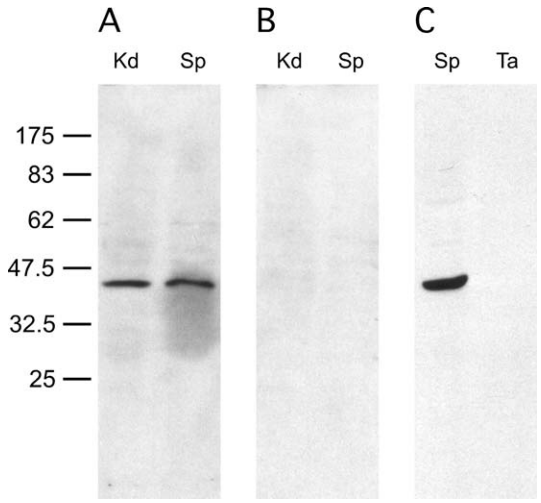

FIG. 1. SORD is present in sperm but not in SDS-insoluble accessory structures of tails. Proteins (10 μg per lane) from kidney (Kd), epididymal sperm (Sp), and SDS-insoluble accessory structures of tails (Ta) were prepared and processed for immunoblot analysis. An immunoreactive band of the predicted size for SORD was present in both kidney and sperm samples. The SORD signal was not detected in SDS-insoluble tails. **A**) Immunoblot probed with anti-SORD polyclonal antibody. **B**) Normal goat IgG. **C**) Anti-SORD polyclonal antibody. Numbers to the left of the figure represent molecular weights of standard proteins ($\times 10^{-3}$).

Gel Electrophoresis and Immunoblot Analyses

The sperm and sperm tails were concentrated by centrifugation, washed in 1 ml of PBS, resuspended in sample buffer (62.5 mM Tris-HCl, pH 6.8, 1.67 % SDS, 10% glycerol), and boiled for 5 min. Kidney tissue was homogenized, sonicated, and boiled in the sample buffer. After centrifuging, the supernatants were saved. The protein concentration was determined by the bicinchoninic acid protein assay (Pierce Chemical Company, Rockford, IL). Subsequently, dithiothreitol (DTT) and bromophenol blue were added to a final concentration of 100 mM and 0.002%. The samples were boiled for 5 min, and 10 μg of protein samples were separated by SDS-PAGE in 10% polyacrylamide gels [22]. The gels were then transferred to polyvinylidene fluoride membranes (Millipore, Bedford, MA) [23], which were blocked with Tris-buffered saline-Tween (TBST; 25 mM Tris-HCl, pH 8.0; 125 mM NaCl; 0.1% Tween 20) containing 5% BSA and incubated with primary antibody (goat anti-mouse SORD IgG [Imgenex, San Diego, CA], 0.5 μg/ml in 5% BSA-TBST). After washing with TBST, the blots were incubated with secondary antibody (donkey anti-goat IgG conjugated with horseradish peroxidase [Santa Cruz Biotechnology, Santa Cruz, CA], 0.08 μg/ml in 5% BSA-TBST) and the bound enzyme was developed with the enhanced chemiluminescence (ECL) kit (GE Healthcare, Buckinghamshire, U.K.), according to the manufacturer's directions, and exposed to film.

To test the extractability of SORD, 10^7 sperm were extracted with one of three solutions: 50 μl ice-cold PBS solution (155.17 mM NaCl, 1.06 mM KH_2PO_4, 2.97 mM Na_2HPO_4-$7H_2O$, pH 7.4), 1% Triton X-100, or 1% SDS-EDTA. After centrifugation of the extracted sperm, the supernatants and pellets were collected. To each 50 μl supernatant, 10 μl 6× sample buffer (375 mM Tris-HCl, pH 6.8, 10% SDS, 30% glycerol, 600 mM DTT, and 0.012% bromophenol blue) was added, and to each pellet was added 50 μl 1× sample buffer (62.5 mM Tris-HCl, pH 6.8, 1.67% SDS, 5% glycerol, 100 mM DTT, and 0.002% bromophenol blue). Each sample was vortexed and boiled for 5 min. Aliquots of each sample (10 μl) were separated by SDS-PAGE in 10% polyacrylamide gels and analyzed by immunoblotting, as described above.

Indirect Immunofluorescence Analyses

Epididymal sperm were collected, mixed by pipette, washed once with PBS, attached to slides, and fixed with 4% paraformaldehyde in PBS for 15 min. After washing with PBS, the sperm were permeabilized with −20°C methanol for 2 min (or without methanol treatment to observe the plasma membrane localization). The slides were washed with PBS and the samples were incubated with 10% horse serum in PBS (blocking solution) for 60 min at room temperature and then with the mixed solution of primary antibodies (5 μg/ml goat anti-SORD antibody; 3.9 μg/ml mouse monoclonal anti-α-tubulin antibody [T5168; Sigma, St. Louis, MO]) in blocking solution for 1 h at room temperature. For a control, equivalent amounts of normal goat IgG and mouse IgG were substituted for the primary antibody mixture. After washing with PBS, the samples were incubated with a mixture of secondary antibodies (1 μg/ml each of rabbit anti-goat IgG and rabbit anti-mouse linked with Alexa Fluo-488 and -568, respectively [Molecular Probes, Eugene, OR]) in blocking solution for 1 h at room temperature. After washing with PBS, the samples were mounted with coverslips using Fluoromount-G (Southern Biotechnology Associates, Inc., Birmingham, AL), examined using an inverted microscope (Nikon Eclipse TE 2000-U, Nikon Corp.) and photographed with a Scion Corporation CFW-1610C digital FireWire camera using the NIH ImageJ Imaging Software [24].

TABLE 1. Parameter settings used with the Hamilton Thorne IVOS software, version 12.2L for mouse for CASA analysis.

Parameter	Setting
Image capture	
Frame per second	60 Hz
No. of frame	30
Cell detection	
Minimum contrast	30
Minimum size	4 pix
Progressive cells	
Average path velocity (VAP)	50.0 μm/sec
Straightness (STR)	50%
Defaults (if <5 motile cells)	
Cell size	13 pix
Cell intensity	75
Slow Cell	
VAP cutoff	10.0 μm/sec
Straight line velocity (VSL) cutoff	0.0 μm/sec
Sort parameter for hyperactive sperm	
Curvilinear velocity (VCL)	>180 μm/sec
Amplitude of lateral head (ALH)	>9.5 μm
Mean linearity (LIN)	<38%

Immunoelectron Microscopy

For immunoelectron microscopy, sperm were isolated and fixed with 4% paraformaldehyde and 0.25% glutaraldehyde. The samples were embedded in Lowicryl K4M that was then polymerized with ultraviolet light (365 nm) for 5 days. Ultrathin sections were cut and mounted on nickel grids coated with Formvar. To prevent nonspecific binding, grids were incubated with blocking buffer (PBS with 1% BSA and 2% normal horse serum) for 30 min at room temperature. The sections were incubated with primary antibody (anti-SORD antibody at 10 μg/ml in blocking buffer or an equal amount of normal goat IgG for negative control) for 1 h at room temperature, washed in buffer, and incubated with 10 nm gold particle-labeled anti-rabbit IgG (2.51 μg/ml in blocking buffer; Ted Pella, Inc., Redding, CA). After incubation at room temperature for 1 h, the grids were rinsed with buffer followed by deionized water for 3 min, air dried, and then examined with a FEI Tecnai G2 electron microscope. Images were collected with a Gatan Camera (Gatan, Inc., Pleasanton, CA).

Sperm Incubation with Sorbitol and Computer-Assisted Semen Analysis

Cauda epididymal sperm were released into a PBS solution (155.17 mM NaCl, 1.06 mM KH_2PO_4, 2.97 mM Na_2HPO_4-$7H_2O$, pH 7.4) as described before, but no centrifugation was utilized for the sperm motility assay. Caudae epididymides were dissected, minced, and incubated at 37°C. After 5 min, the adequate dispersion of the sperm was determined visually. The sperm supernatant was aspirated and the sperm concentration was counted with a hemocytometer. The final sperm concentration was adjusted to 2.0×10^6 sperm/ml. Sorbitol, glucose, or fructose in stock solutions of 1 M in PBS were individually added to 200 μl sperm aliquots to a final concentration of 5 mM. In the no-sugar control samples, NaCl was added for a final concentration of 2.5 mM to control for osmolarity differences between the experimental and control samples. Aliquots were analyzed using computer-assisted semen analysis (CASA) (Hamilton-Thorne IVOS V12.2L; Hamilton-Thorne Research, Danvers, MA). CASA measurements were obtained after 0, 60, 120, 180, and 240 min of incubation. Videos of the sperm were taken to document sperm motility at the 1 h and 4 h time points. To further evaluate the effect of sorbitol on sperm

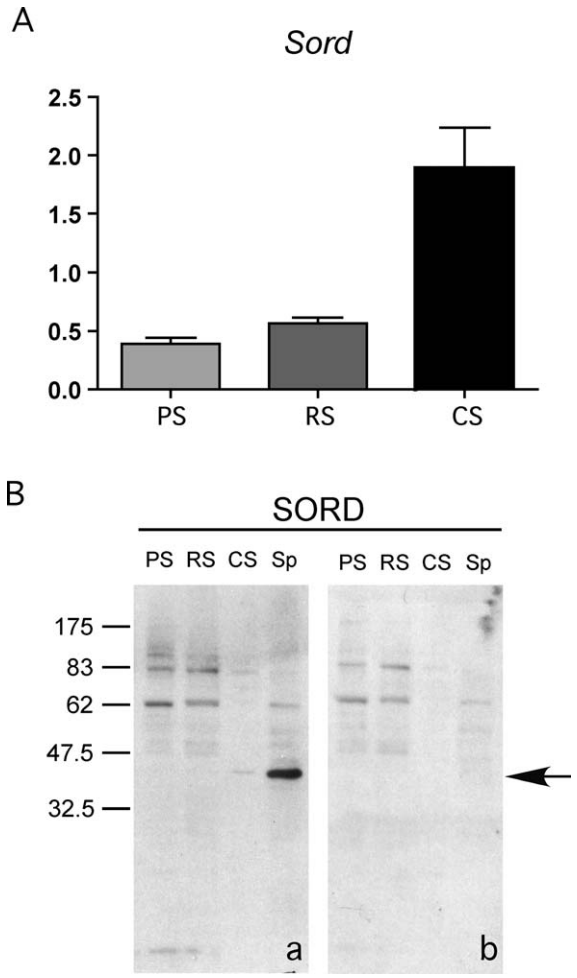

FIG. 2. *Sord* mRNA and its encoded protein are highly expressed at the end stage of spermiogenesis; SORD protein becomes more abundant in condensing spermatids and epididymal sperm. **A**) Quantitative RT-PCR of *Sord* from pachytene spermatocytes (PS), round spermatids (RS), and condensing spermatids (CS). Results were normalized to mRNA corresponding to ribosomal protein S16. **B**) Immunoblot analysis of SORD (arrow) from pachytene spermatocytes (PS), round spermatids (RS), condensing spermatids (CS), and epididymal sperm (Sp). **a**) Anti-SORD polyclonal antibody. **b**) Normal goat IgG. The arrow indicates the specific SORD band. Please note: to see the weak signal of SORD in condensing spermatids, the film is overexposed. Therefore, some weak background bands appeared (also present in control), compared with Figure 1. Numbers to the left of the figure represent molecular weights of standard proteins ($\times 10^{-3}$).

motility, either sorbitol and the glycolytic pathway inhibitor alpha-chlorohydrin (ACH; final concentrations of 5 mM and 10 mM, respectively) or sorbitol alone (5 mM final concentration with 5 mM NaCl to control for the osmolality difference) were added to 200-μl aliquots of a sperm suspension in PBS [25, 26]. Sperm motility was measured at 0, 15, 30, 60, and 120 min by CASA. The CASA analysis was done as follows. Sperm aliquots (5 μl) were placed on a prewarmed, 20-μm-depth counting chamber slide (Leja Products, The Netherlands). The CASA motility parameters used were those recommended by the manufacturer for mouse sperm (see Table 1).

Capacitation of Spermatozoa, Protein Preparation, and Measurement of Hyperactive Sperm Motility

For experiments in which protein tyrosine phosphorylation was assessed, sperm were collected and incubated under capacitating conditions as described by Travis et al. [27]. Briefly, sperm were allowed to swim out from the caudae epididymides into 2 ml of modified Whitten medium (ModW: 22 mM HEPES, 1.2 mM $MgCl_2$, 100 mM NaCl, 4.7 mM KCl, 1 mM pyruvic acid, 4.8 mM lactic acid hemi-calcium salt, pH 7.35) at 37°C. Epididymal tissue was removed, and the sperm were washed at 100 × *g* for 1 min in a clinical centrifuge to remove any gross tissue debris. The sperm were resuspended in a final volume of 3–8 ml of ModW, and then centrifuged at 500 × *g* for 8 min in a round-bottomed tube. The resultant "fluffy" pellet was counted, assessed for motility, and diluted for use. In all cases, large-bore plastic transfer pipettes or large-orifice pipette tips were used to minimize damage to the sperm membranes. After collection and washing, sperm were incubated under noncapacitating (ModW medium with respective monosaccharide) or capacitating conditions (ModW with 10 mM $NaHCO_3$, 3 mM 2-hydroxypropyl-b-cyclodextrin [2-OH-β-CD], and respective monosaccharide), and capacitation conditions without monosaccharide (ModW with 10 mM $NaHCO_3$, and 3 mM 2-OH-β-CD) for 1.5 h in a 37°C water bath at a final concentration of 4×10^6 sperm in 600 μl. To use a completely defined medium, 2-OH-β-CD was used as a cholesterol acceptor in place of BSA. Depending upon the experiment, the sperm were incubated with sorbitol, glucose, or fructose as metabolic substrates. Sperm were then concentrated by centrifugation at 10 000 × *g* and then washed in 1 ml of ModW containing 0.2 mM Na_3VO_4 to inhibit phosphatase activity during extraction. Sperm were centrifuged at 10 000 × *g* again, and the pellet was suspended in 50 μl 1× sample buffer (62.5 mM Tris-Cl, pH 6.8, 10% glycerol, 1.67% SDS, 100 mM DTT, 0.002% bromophenol blue). The samples were boiled at 100°C for 5 min and spun at 10 000 × *g*. The supernatant was ready for subsequent electrophoresis.

For experiments measuring sperm hyperactive motility, all steps were similar, except that the sperm from 2–3 mice were suspended in 0.5 ml. No centrifugation was needed. The final sperm concentration was adjusted to 2×10^6 sperm in 300 μl. Samples of sperm (5 μl) were removed for CASA analysis after 1.5-h incubation, as described above. Hyperactivated motility was defined as motility with high-amplitude thrashing patterns and short trajectory distances. The criteria for detecting hyperactivated spermatozoa were VCL >180 μm/sec, ALH > 9.5 μm, and LIN < 38% [28]. The increase in hyperactive motility was calculated by subtracting the baseline hyperactive motility measured at 0 min of incubation.

Detection of Protein Tyrosine Phosphorylation

Supernatant aliquots (10 μl) were separated under reducing conditions by SDS-PAGE in 10% polyacrylamide gels. Detection of tyrosine phosphorylation was achieved by immunoblotting after transfer to Immobilon-P membranes (Millipore). Membranes were blocked for at least 1 h in PBS containing 0.1% Tween 20 (PBST) and 5% cold-water fish gelatin (Sigma), and washed three times in PBST for 5 min, probed overnight with anti-phosphotyrosine mouse monoclonal antibody 4G10 (0.1 μg/ml in PBST; Upstate Biotechnology, Billerica, MA). Blots were then washed three times in PBST for 5 min before being incubated for 1 h with donkey anti-mouse IgG conjugated with horseradish peroxidase (1:5000 dilution in PBST; GE Healthcare). Blots were washed three times in PBST for 5 min and then detected with the ECL kit (GE Healthcare) according to the manufacturer's directions, and exposed to film.

Quantitative PCR Analyses

For quantitative RT-PCR assays, primers were designed using Primer Express 1.5 Taqman Primer Design software (Applied Biosystems, Foster City, CA). The *Sord* primers, 5′-TGG GAG CTG CTC AAG TTG TG-3′ (forward) and 5′-GGT CTC TTT GCC AAC CTG GAT-3′ (reverse), were used at a working concentration of 22.5 nM and yielded a product of 100 bp. The ribosomal protein S16 (*Rps16* [GenBank accession number: BC082286]) primers, 5′-AGA TGA TCG AGC CGC GC-3′ (forward) and 5′-GCT ACC AGG GCC TTT GAG ATG GA-3′ (reverse), were used at a working concentration of 11.25 nM and yielded a product of 163 bp [29]. Products were amplified with the SYBR Green PCR Master Mix and analyzed with the ABI 7900 HT Sequence Detection system. The following PCR protocol was used: 1) denaturation (50°C for 2 min, 95°C for 10 min), 2) amplification and quantification (95°C for 15 sec, 60°C for 1 min) repeated for 40 cycles, 3) a dissociation curve program (95°C for 15 sec, 60°C for 15 sec, 95°C for 15 sec), and 4) cooling at 4°C. Amplicons were analyzed by generating a dissociation curve and determining the threshold cycle (Ct) value for each transcript. The relative quantification of gene expression was analyzed by the $2^{-\Delta\Delta C_T}$ method [30]. The mRNA corresponding to Rps16 was used as a control [29].

Statistical Analysis

Data were expressed as means ± SEM and compared by one-way ANOVA and Student-Newman-Keuls multiple comparison test. Statistical analyses were performed using the GraphPad Prism program (GraphPad Software, San Diego, CA).

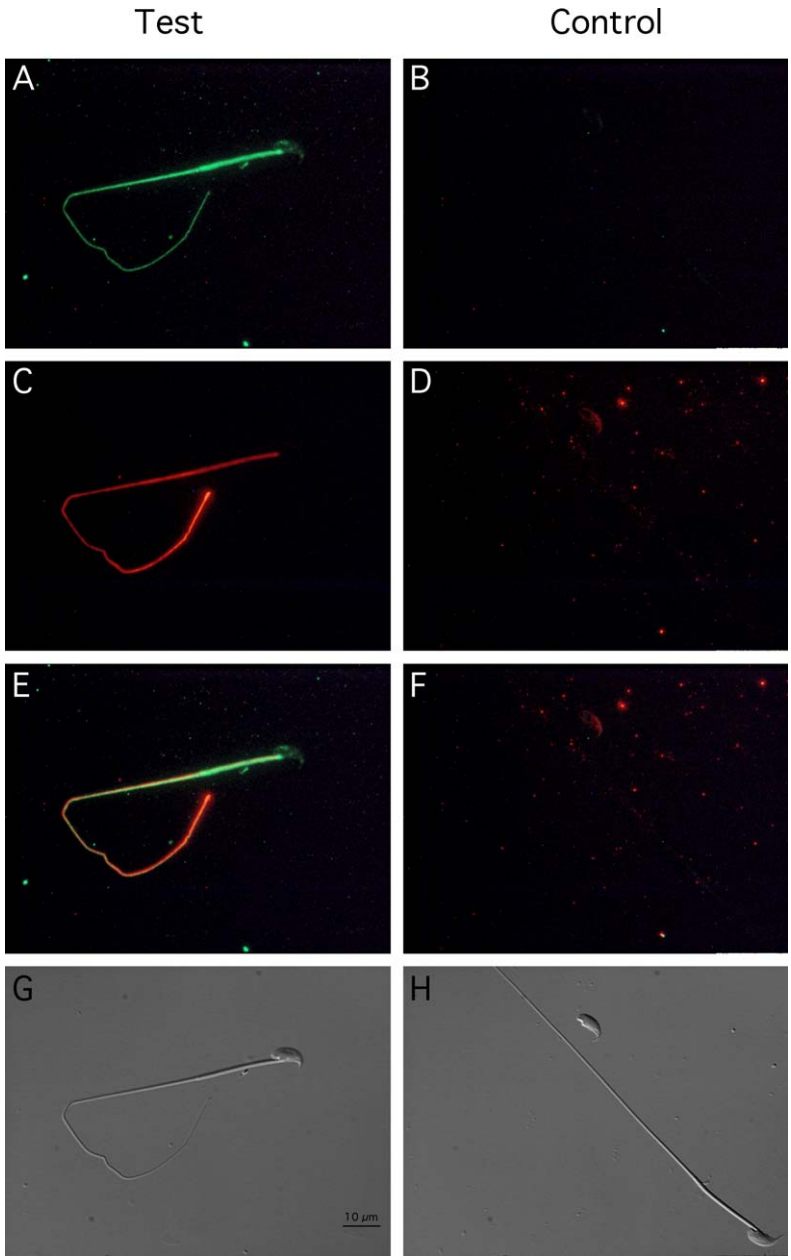

FIG. 3. SORD is present along the entire length of sperm flagellum, but does not show the same distribution pattern as α-tubulin. Indirect immunofluorescence of sperm probed with anti-SORD antibody (**A**), normal goat IgG (**B**), monoclonal antibody to α-tubulin (**C**), and normal mouse IgG (**D**). **E**) Merged image of **A** and **C**. **F**) Merged image of **B** and **D**. **G**) Corresponding Nomarski differential interference contrast image of test group. **H**) Corresponding Nomarski image of control group. Bar = 10 μm.

RESULTS

Mouse Sperm SORD

We determined that SORD was present in mouse sperm by immunoblotting (Fig. 1, A and B). A single band with the expected molecular weight of approximately 39 000 kDa was identified in mouse sperm; a similar-sized band was found in kidney protein, which was used as a positive control. No signal was detected in the control blot, probed with an equal amount of normal goat IgG, demonstrating that the signal in Figure 1A was specific for SORD. We further examined whether this enzyme was part of sperm accessory structures, composed of the mitochondrial sheath, outer dense fibers, and fibrous sheath (Fig. 1C). The purified accessory structure was examined visually under light microscope (see Supplemental Fig. S1) and by immunoblotting and immunoelectron microscopy [20, 21]. Equal amounts of sperm and purified sperm accessory structure protein were analyzed by SDS-PAGE. No signal was detected in the latter sample, indicating that SORD either was lost during sample preparation because it was not tightly associated with the sperm accessory structures, or that it was not present. Since 1% SDS (S-EDTA) used in purifying accessory structures might extract some proteins from the outer dense fibers, fibrous sheath, or the mitochondrial sheath, milder extraction conditions were used to confirm the previous findings. Ice-cold PBS or 1% Triton X-100 was utilized to extract protein from sperm. As demonstrated by immunoblotting, SORD was easily extracted from sperm, even with ice-cold PBS. Almost all of the SORD could be extracted into the supernatant with 1% Triton X-100 (see Supplemental Fig. S2).

Sord *mRNA and SORD Protein Expression Up-Regulated During Late Spermiogenesis*

To examine the expression pattern of *Sord* mRNA in germ cells, quantitative real-time PCR was conducted (Fig. 2A). *Sord* mRNA was present in pachytene spermatocytes, round

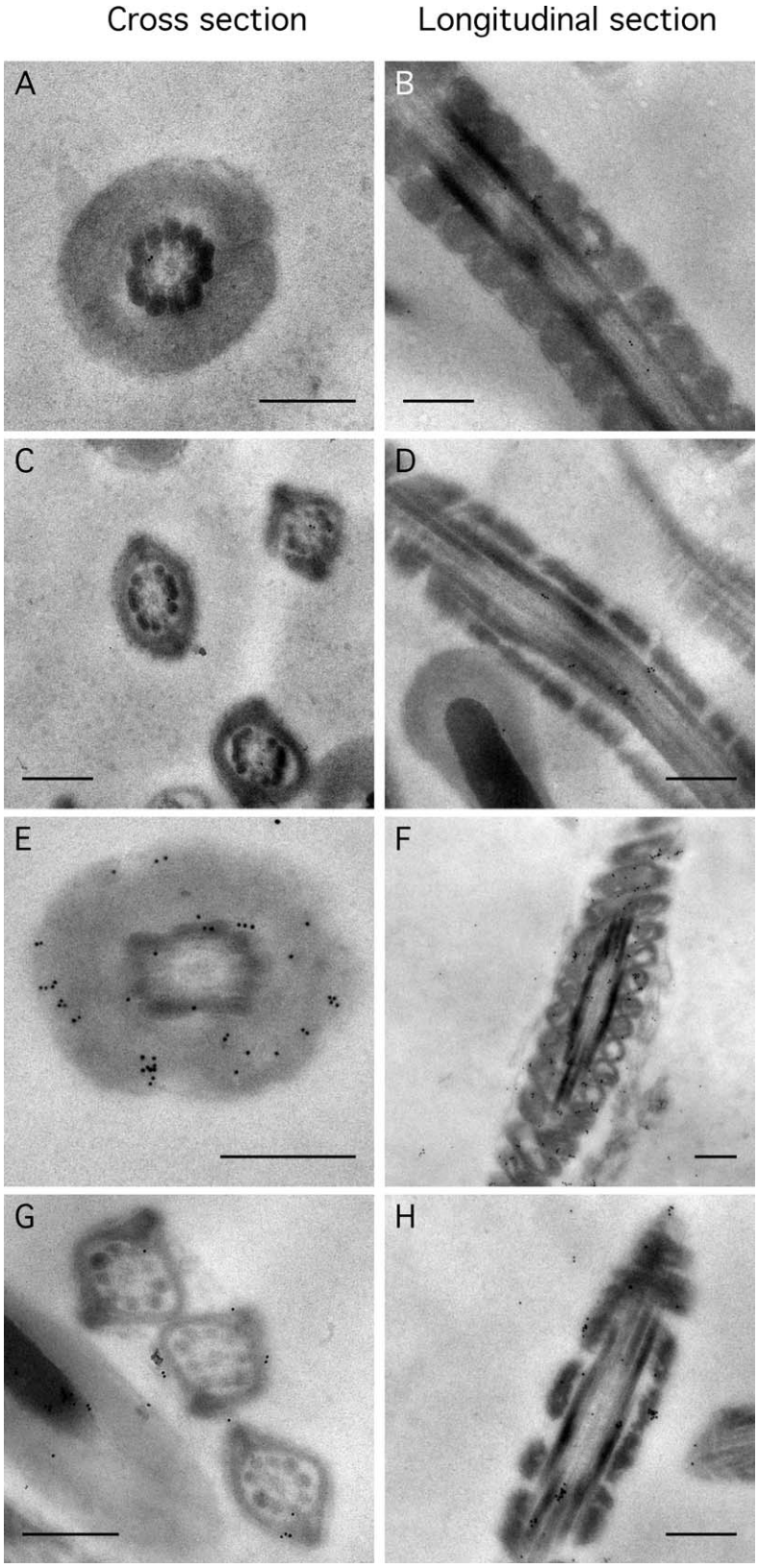

FIG. 4. SORD is associated with mitochondria and near the plasma membrane of the sperm flagellum. Immunoelectron microscopy of cross sections of sperm (left column) and longitudinal sections (right column) of similar regions. **A**, **B**, **E**, and **F** are views of the midpiece. **C**, **D**, **G**, and **H** are sections of the principal piece. Sperm sections in **A**–**D** were probed with normal goat IgG. Sections in **E**–**H** were probed with anti-SORD polyclonal antibody. Bar = 0.5 μm.

spermatids, and condensing spermatids. However, the level was higher in condensing spermatids (>3-fold), compared to pachytene spermatocytes. Expression results at the protein level suggested that the translation of the *Sord* mRNA was regulated, since SORD protein was first detected by immunoblotting in condensing spermatids (Fig. 2B). The finding that the signal intensity in condensing spermatids was not as high as was found for sperm can be largely explained because the condensing spermatids recovered from the purification procedure have lost their flagella as a result of the trypsinization step used to disperse the seminiferous tubules into a single cell suspension.

A

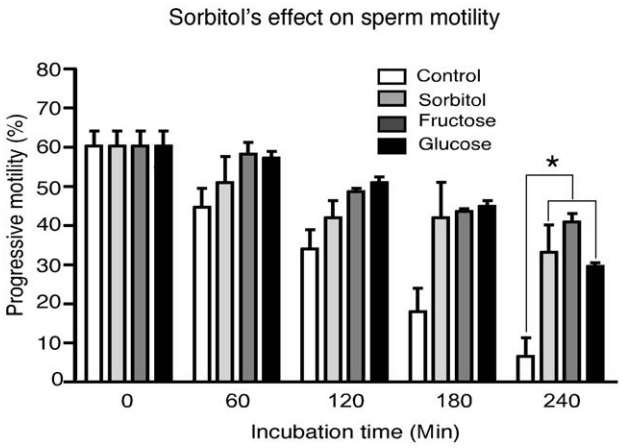

B

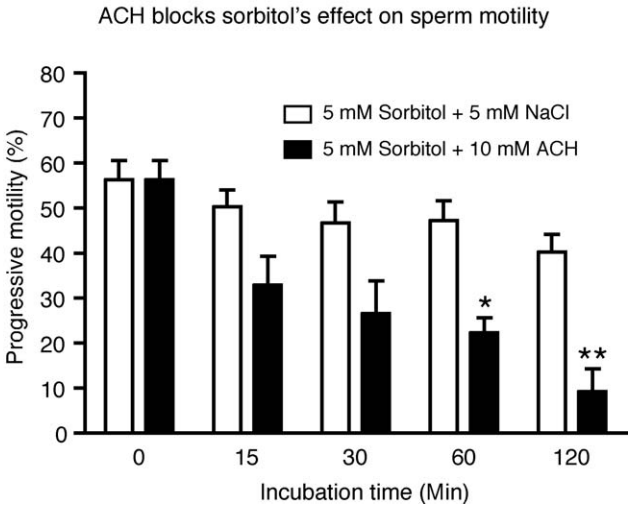

FIG. 5. Sorbitol helps maintain sperm motility during incubation. Motility of sperm incubated in PBS with NaCl (control), sorbitol, fructose, or glucose was measured by computer-assisted semen analysis (CASA) at different time points. Three experiments were performed, and the results were reproducible. This figure demonstrates the changes over the course of incubation: **A**) The progressive sperm percentage of total sperm ($n = 3$; $^*P < 0.05$). **B**) ACH effect on sperm motility maintained by sorbitol ($n = 3$; $^*P < 0.05$, $^{**}P < 0.01$).

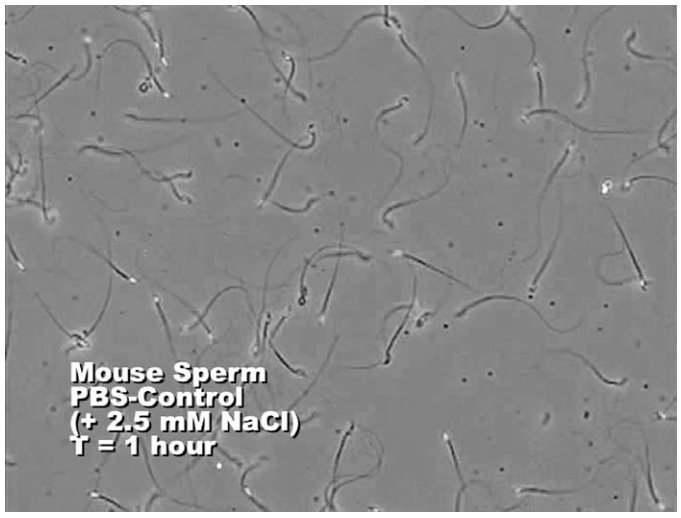

FIG. 6. Sperm were incubated in PBS with an additional 2.5 mM NaCl (control) or with 5 mM sorbitol added (experimental). Sperm progressive motility patterns were measured by CASA and recorded as videos. This image is a still from a composite video (see Supplemental Movie available online at http://www.biolreprod.org) of the various treatments presented in the following sequence: control at 1 h, experimental at 1 h, control at 4 h, and experimental at 4 h.

SORD Present along the Full Length of the Sperm Flagellum in Two Subcompartments

To compare the subcellular localization of SORD with the axoneme, which runs the full length of the sperm flagellum, we detected SORD by immunofluorescence concurrently with α-tubulin (Fig. 3). Although both SORD and α-tubulin were found throughout the entire length of sperm flagellum (Fig. 3, A and C), their respective signal intensities were distributed differently (Fig. 3E). SORD immunofluorescence demonstrated more intense signals in the midpiece, whereas axonemal α-tubulin showed stronger fluorescence in the distal region of the flagellum, probably because the antibody had a greater accessibility to the axoneme due to the absence of accessory structures in the end piece. To clarify whether SORD is on the membrane or in cytoplasm, sperm without methanol treatment were probed with anti-SORD antibody. The signal was detected along the entire length of the sperm tail (see Supplemental Fig. S3).

To refine the subcellular localization of SORD, immunoelectron microscopy was conducted. Normal goat IgG was used as a control, which demonstrated that negligible numbers of nonspecific binding gold particles mainly appeared around the outer dense fibers in both the midpiece and principal piece (Fig. 4, A–D). When probed with the anti-SORD antibody, numerous gold particles were associated with mitochondria of the midpiece (Fig. 4, E and F) and near the plasma membrane in the principal piece of the flagellum (Fig. 4, G and H).

Sorbitol Support of Sperm Motility

Fructose has been demonstrated to be an energy source for sperm. Since SORD is involved in fructose synthesis by the polyol pathway, we hypothesized that SORD could support sperm motility. However, few experiments have been done to evaluate the role of SORD in sperm motility. Here, we applied CASA of sperm incubated with sorbitol to determine its effect on motility. To exclude any other energy source, PBS was chosen as the sperm medium. The results showed that sorbitol, as well as glucose and fructose, were able to maintain sperm motility longer than 4 h, whereas most sperm without an added energy source were immotile by this time point (Fig. 5A). The motility decrease was significantly different ($P < 0.05$). Sperm incubated without monosaccharide exhibited progressive motility for at least 1 h (see Fig. 6 and Supplemental Movie), but most of the sperm were immotile after a 4-h incubation. However, sperm incubated with sorbitol maintained substantial motility by 4 h. When ACH, a blocker of glycolytic pathway [26], was added to the sperm cultured with 5 mM sorbitol, the sperm motility decreased dramatically (Fig. 5B; $P < 0.01$). Sorbitol and fructose can also replace glucose in sperm capacitating medium, which showed about a 5%–10% increase of hyperac-

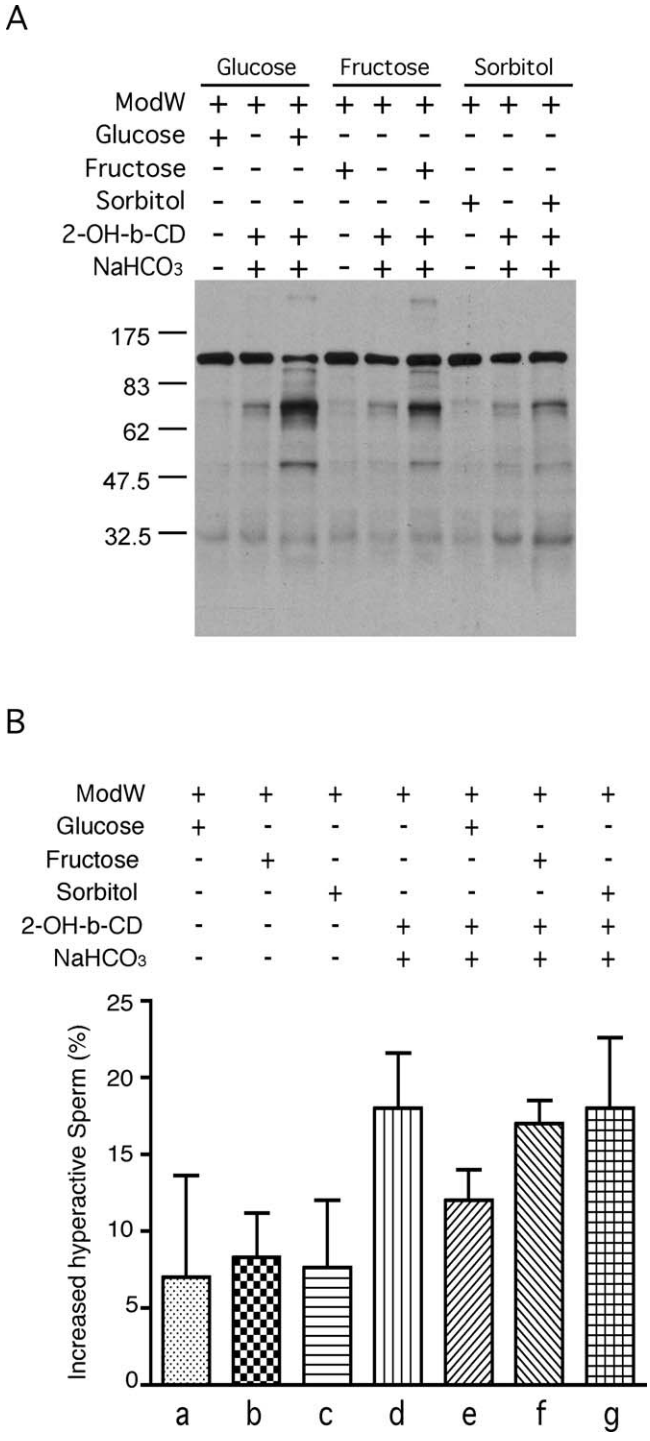

FIG. 7. Sorbitol can substitute for glucose or fructose in capacitating media. Sperm were incubated in noncapacitating medium (ModW with monosaccharide), regular capacitating medium (ModW with monosaccharide, sodium bicarbonate, 2-OH-β-CD [labeled as 2-OH-b-CD]), or regular capacitating medium lacking monosaccharide for 1.5 h. **A**) Sperm proteins were extracted, subjected to SDS-PAGE, immunoblotted, and probed with anti-phosphotyrosine antibody. This experiment was repeated twice with similar results. Numbers to the left of the figure represent molecular weights of standard proteins ($\times 10^{-3}$). **B**) Hyperactive motility was measured among the different groups above. Increased hyperactive motility was normalized by subtracting baseline hyperactive motility (at time point 0). The sperm were incubated in noncapacitating media (with glucose [a], fructose [b], sorbitol [c]) or in capacitating medium (with no added sugar [d], glucose [e], fructose [f], sorbitol [g]) (n = 3).

tive sperm percentage compared with the noncapacitating control group. However, sperm incubated in capacitating medium without any added monosaccharide also exhibited a 10% increase in hyperactive motility (Fig. 7B). The increase in hyperactive motility is similar to the values reported in other studies, although the solutions used are different [31, 32].

Sorbitol Incubation Leads to Increased Protein Tyrosine Phosphorylation

To examine the role of sorbitol in sperm function, we explored whether sorbitol is able to support sperm protein tyrosine phosphorylation. One striking hallmark of the process of sperm capacitation is an overall increase in protein tyrosine phosphorylation compared with noncapacitated sperm. We divided the sperm sample into three groups to see the effects of glucose, fructose, and sorbitol (5 mM each) on sperm capacitation. Incubation of sperm under capacitating conditions with any one of the three monosaccharides clearly resulted in much higher protein tyrosine phosphorylation signals than were found for noncapacitated sperm. Moreover, among the three capacitation groups, sperm incubated with glucose showed a stronger signal than those with either fructose or sorbitol. In addition, the capacitation-associated increase in protein tyrosine phosphorylation was dependent upon the addition of monosaccharide; as has been previously found for glucose, if we omitted either fructose or sorbitol, the tyrosine phosphorylation signals decreased dramatically in each case (Fig. 7A).

DISCUSSION

Sorbitol and Sperm Physiology

Although sorbitol has long been known to be present in male and female reproductive tract fluids, a direct connection between sorbitol and sperm function has not been established. Our studies show that sperm were able to utilize sorbitol as an energy source to maintain baseline motility (Figs. 5A and 6; Supplemental Movie). Sperm incubated for 1 h in control PBS or 5 mM sorbitol were still quite mobile. This may have been partially due to the fact that the sperm were not centrifuged and may have carried some epididymal energy sources along with them to the assay. However, any energy sources emanating from the epididymal fluid would have been equally distributed to both the control and experimental samples. By 4 h, the control sperm were almost all immotile, but the sperm kept in 5 mM sorbitol maintained a high level of motility.

Sperm capacitation is related to acrosomal exocytosis, sperm hyperactive motility, protein tyrosine phosphorylation, etc. Our results show that sorbitol increased the level of protein tyrosine phosphorylation (Fig. 7A). Our findings suggest that carbohydrates other than glucose may be able to fulfill the role of an energy source for this process. Although our results show that sorbitol could increase tyrosine phosphorylation levels when replacing glucose in capacitating conditions, this polyol was not able to induce as robust a tyrosine phosphorylation response as did glucose or fructose, possibly because sorbitol needs to be converted into fructose to enter the metabolic pathway. On the other hand, these phenomena indicate that mouse sperm utilize glucose more efficiently than other monosaccharides at the same concentration (Fig. 7A). It is likely that sperm from other species may show differential tyrosine phosphorylation in response to various sugars or sugar alcohols. Sorbitol can replace glucose as a component in the medium used for sperm capacitation and lead to an increase in protein tyrosine phosphorylation similar to that seen with glucose. However, monosaccharides might not be important

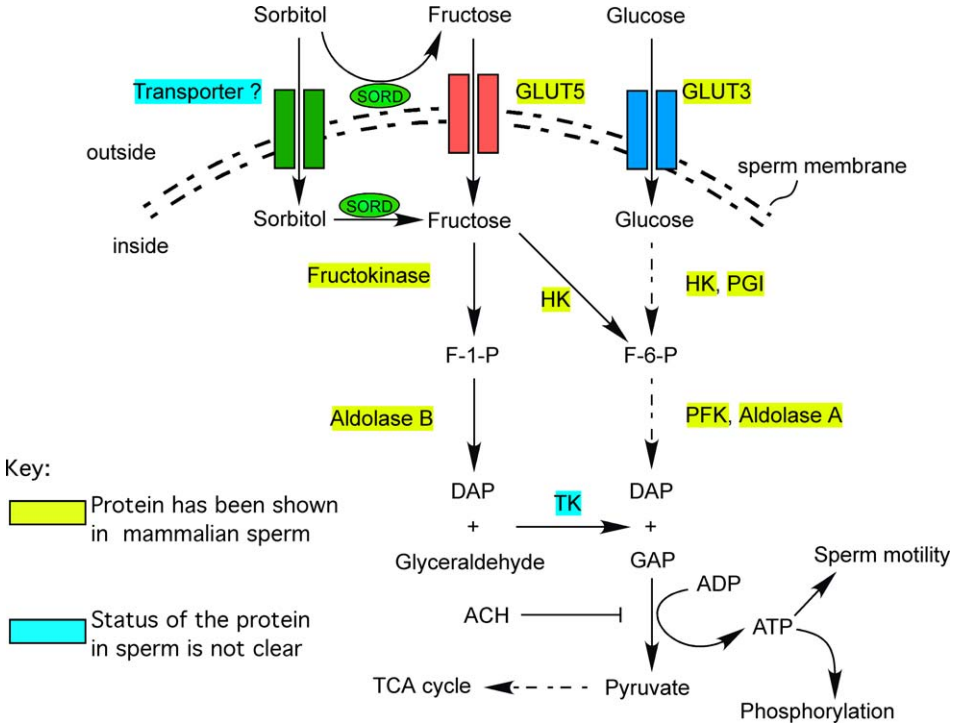

FIG. 8. Sorbitol can act as an alterative energy source for sperm motility and signal transduction in proposed metabolic pathway. ACH blocks glyceraldehyde 3-phosphate dehydrogenase. DAP, dihydroxyacetone phosphate; F-1-P, fructose 1-phosphate; F-6-P, fructose 6-phosphate; GAP, glyceraldehyde 3-phosphate; GLUT, glucose transporter; HK, hexokinase; PFK, phosphofructokinase; PGI, phosphoglucose isomerase; SORD, sorbitol dehydrogenase; TCA, citric acid cycle; TK, triokinase.

factors in the initiation and maintenance of hyperactive motility (Fig. 7B), since a "capacitating" medium lacking sorbitol, glucose, or fructose can achieve similar levels of hyperactive motility. In particular, 2-OH-β-CD and/or $NaHCO_3$ could be important factors for the observed increase in hyperactive motility.

Sorbitol Dehydrogenase Expression and Localization

Few studies have looked at the expression and localization of SORD in male reproductive tissues [8, 14–16]. Quantitative RT-PCR demonstrated that *Sord* mRNA was present early in spermatogenesis in the meiotic pachytene spermatocytes (Fig. 2A). However, SORD protein was first detectable in postmeiotic haploid condensing spermatids, suggesting that a post-transcriptional delay in protein synthesis exists (Fig. 2B). By using in situ hybridization and immunohistochemistry of rat and mouse testes, other groups also reported that *Sord* mRNA and protein levels were found to rise over the course of germ cell differentiation [8, 14]. One immunocytochemical study was performed on rat sperm, showing that the entire sperm stained evenly [8]. Our results in the mouse, however, demonstrate that the SORD signal is found mainly in the sperm flagellum, and that there is negligible staining in the sperm head. This discrepancy in localization in rat and mouse sperm might be due to a difference between species. Since tubulin is the major protein in the axoneme, the fact that SORD and tubulin displayed immunofluorescence signal intensity differences along the length of the flagellum suggests that SORD is not an axonemal protein (Fig. 3). Based on the distribution pattern of SORD, it is also unlikely that SORD is a part of a flagellar accessory structure, because the end piece, which contains only the axoneme enclosed by the plasma membrane, was also stained. SORD signal could also be detected in the full length of sperm tail without pretreatment of methanol (see Supplemental Fig. S3). These results suggest that some SORD is associated with the plasma membrane. In addition, in comparison to whole mouse sperm, the SORD immunoblotting signal in isolated flagellar accessory structures was not abundant. This indicates that SORD is not a component of the accessory structures, or that it is not tightly bound to the fibrous sheath or outer dense fibers, as is the case with hexokinase [27] (Fig. 1). SORD was also readily extracted by ice-cold PBS and 1% Triton X-100, which further supports our conclusion that SORD is not associated with flagellar accessory structures (Supplemental Fig. S2). Utilizing immunoelectron microscopy, we found SORD signals near the plasma membrane and also in association with mitochondria (Fig. 4, E and G). We also observed that the gold particles were not randomly distributed, nor were they detected in the negative control, demonstrating that the gold particles were binding specifically to the mitochondria.

A vesicle called epididymosome [33, 34], secreted by the epididymal epithelium in an apocrine manner, has been shown to be a carrier of SORD by immunoblotting [15]. Furthermore, epididymosomes transfer proteins, such as p25b, from the epididymal fluid to the sperm surface [35]. Thus, it is likely that SORD may also be transferred to the sperm surface. As a result, SORD in sperm could be derived from two sources: the progenitor germ cell or an exogenous source, such as the epididymal epithelium.

Sorbitol Metabolic Pathway in Sperm

Sorbitol, unlike glucose and fructose, is a linear molecule, which makes it difficult to penetrate eukaryotic cell plasma membranes [36]. With SORD near the sperm plasma membrane, the enzyme will be able to convert sorbitol into fructose [37]. The glucose transporter isoform, glucose transporter 5, officially known as SLC2A5, has been shown to function also as a fructose transporter, and has been localized to the plasma membrane of mature spermatozoa, including the entire sperm flagellum [38]. As a consequence, the transporter could move sorbitol-derived fructose into sperm, which could then be used as an energy source for glycolysis and oxidative phosphorylation. In addition, there have been several reports showing, by radiochemical methods, that sperm can take up fructose [39, 40]. Another possibility is

that sorbitol could be transported into the sperm by a specific transporter. This kind of transporter has been cloned from bacteria, and other studies have indicated that there is a sorbitol transport system in renal interstitial cells [41, 42]. Inside sperm, fructose can be converted to fructose 1-phosphate by hexokinase to enter the glycolytic pathway. In addition, most enzymes in fructose metabolism have also been reported to be present in the mammalian sperm flagellum, indicating that fructose metabolic pathways may be operative [43–48] (Fig. 8). By these paths, SORD could promote the use of sorbitol as an alternative energy source. The ability of sorbitol to support sperm motility is blocked by ACH, indicating that sorbitol produces energy through the glycolytic pathway (Fig. 5B).

Future Directions

Many aspects of the functional significance of sorbitol and SORD in sperm remain unclear. The role of sorbitol in acrosomal exocytosis, as well as sperm-egg interactions, must still be determined. Although SORD-deficient mice do not demonstrate a significant fertilization defect [49], compensation for the missing SORD activity at the enzyme level or the reduced sugar level in the reproductive tract have not been determined. In addition, complete blockage of the SORD enzymatic reaction might also help reveal the role of SORD in sperm physiology.

ACKNOWLEDGMENTS

Immunoelectron microscopy was performed by the BioMedical Imaging Facility at the University of Pennsylvania. We thank Dr. Qianchun Yu and Neelima Shah of this facility for their expertise and guidance during the course of these studies. We also thank members of our laboratory for their insights concerning this project.

REFERENCES

1. Palomo MJ, FernAndez-Novell JM, Pena A, Guinovart JJ, Rigau T, Rodriguez-Gil JE. Glucose- and fructose-induced dog-sperm glycogen synthesis shows specific changes in the location of the sperm glycogen deposition. Mol Reprod Dev 2003; 64:349–359.
2. O'Shea T, Wales RG. Metabolism of sorbitol and fructose by ram spermatozoa. J Reprod Fertil 1965; 10:353–368.
3. Jones AR, Connor DE. Fructose metabolism by mature boar spermatozoa. Reprod Fertil Dev 2000; 12:355–359.
4. Mann T, White IG. Metabolism of glycerol, sorbitol and related compounds by spermatozoa. Nature 1956; 178:142–143.
5. Medrano A, Fernandez-Novell JM, Ramio L, Alvarez J, Goldberg E, Montserrat Rivera M, Guinovart JJ, Rigau T, Rodriguez-Gil JE. Utilization of citrate and lactate through a lactate dehydrogenase and ATP-regulated pathway in boar spermatozoa. Mol Reprod Dev 2006; 73: 369–378.
6. Jones AR. Metabolism of lactate by mature boar spermatozoa. Reprod Fertil Dev 1997; 9:227–232.
7. Jones AR, Chantrill LA, Cokinakis A. Metabolism of glycerol by mature boar spermatozoa. J Reprod Fertil 1992; 94:129–134.
8. Kobayashi T, Kaneko T, Iuchi Y, Matsuki S, Takahashi M, Sasagawa I, Nakada T, Fujii J. Localization and physiological implication of aldose reductase and sorbitol dehydrogenase in reproductive tracts and spermatozoa of male rats. J Androl 2002; 23:674–683.
9. Mann T. Studies on the metabolism of semen: 3. Fructose as a normal constituent of seminal plasma. Site of formation and function of fructose in semen. Biochem J 1946; 40:481–491.
10. King TE, Mann T. Sorbitol metabolism in spermatozoa. Proc R Soc Lond B Biol Sci 1959; 151:226–243.
11. Zaayer D, van der Horst CJ. Non-fertility in cows: influence of PGF, PMSG followed by PGF, progesterone and light. Cytobios 1984; 40:35–60.
12. Kaneko T, Iuchi Y, Takahashi M, Fujii J. Colocalization of polyol-metabolizing enzymes and immunological detection of fructated proteins in the female reproductive system of the rat. Histochem Cell Biol 2003; 119:309–315.
13. King TE, Mann T. Sorbitol dehydrogenase in spermatozoa. Nature 1958; 182:868–869.
14. Lee FK, Lee AY, Lin CX, Chung SS, Chung SK. Cloning, sequencing, and determination of the sites of expression of mouse sorbitol dehydrogenase cDNA. Eur J Biochem 1995; 230:1059–1065.
15. Frenette G, Lessard C, Sullivan R. Polyol pathway along the bovine epididymis. Mol Reprod Dev 2004; 69:448–456.
16. Pruneda A, Pinart E, Bonet S, Yeung CH, Cooper TG. Study of the polyol pathway in the porcine epididymis. Mol Reprod Dev 2006; 73:859–865.
17. Bellvé AR, Millette CF, Bhatnagar YM, O'Brien DA. Dissociation of the mouse testis and characterization of isolated spermatogenic cells. J Histochem Cytochem 1977; 25:480–494.
18. Romrell LJ, Bellvé AR, Fawcett DW. Separation of mouse spermatogenic cells by sedimentation velocity. Dev Biol 1976; 49:119–131.
19. O'Brien DA, Bellvé AR. Protein constituents of the mouse spermatozoon. I. An electrophoretic characterization. Dev Biol 1980; 75:386–404.
20. Cao W, Gerton GL, Moss SB. Proteomic profiling of accessory structures from the mouse sperm flagellum. Mol Cell Proteomics 2006; 5:801–810.
21. Cao W, Haig-Ladewig L, Gerton GL, Moss SB. Adenylate kinases 1 and 2 are part of the accessory structures in the mouse sperm flagellum. Biol Reprod 2006; 75:492–500.
22. Laemmli UK. Cleavage of structural proteins during the assembly of the head of bacteriophage T4. Nature 1970; 227:680–685.
23. Towbin H, Staehelin T, Gordon J. Electrophoretic transfer of proteins from polyacrylamide to nitrocellulose sheets: procedure and some applications. Proc Natl Acad Sci U S A 1979; 76:4350–4354.
24. Rasband WS. ImageJ. National Institutes of Health, Bethesda, Maryland. 2007. World Wide Web (URL: http://rsb.info.nih.gov/ij/).
25. Tanaka H, Takahashi T, Iguchi N, Kitamura K, Miyagawa Y, Tsujimura A, Matsumiya K, Okuyama A, Nishimune Y. Ketone bodies could support the motility but not the acrosome reaction of mouse sperm. Int J Androl 2004; 27:172–177.
26. Bone W, Cooper TG. In vitro inhibition of rat cauda epididymal sperm glycolytic enzymes by ornidazole, alpha-chlorohydrin and 1-chloro-3-hydroxypropanone. Int J Androl 2000; 23:284–293.
27. Travis AJ, Jorgez CJ, Merdiushev T, Jones BH, Dess DM, Diaz-Cueto L, Storey BT, Kopf GS, Moss SB. Functional relationships between capacitation-dependent cell signaling and compartmentalized metabolic pathways in murine spermatozoa. J Biol Chem 2001; 276:7630–7636.
28. Bray C, Son JH, Kumar P, Meizel S. Mice deficient in CHRNA7, a subunit of the nicotinic acetylcholine receptor, produce sperm with impaired motility. Biol Reprod 2005; 73:807–814.
29. Jeong YJ, Choi HW, Shin HS, Cui XS, Kim NH, Gerton GL, Jun JH. Optimization of real time RT-PCR methods for the analysis of gene expression in mouse eggs and preimplantation embryos. Mol Reprod Dev 2005; 71:284–289.
30. Livak KJ, Schmittgen TD. Analysis of relative gene expression data using real-time quantitative PCR and the 2(−Delta Delta C(T)) method. Methods 2001; 25:402–408.
31. Rodriguez-Miranda E, Buffone MG, Edwards SE, Ord TS, Lin K, Sammel MD, Gerton GL, Moss SB, Williams CJ. Extracellular adenosine 5′-triphosphate alters motility and improves the fertilizing capability of mouse sperm. Biol Reprod 2008; 79:164–171.
32. Shao M, Ghosh A, Cooke VG, Naik UP, Martin-DeLeon PA. JAM-A is present in mammalian spermatozoa where it is essential for normal motility. Dev Biol 2008; 313:246–255.
33. Frenette G, Lessard C, Madore E, Fortier MA, Sullivan R. Aldose reductase and macrophage migration inhibitory factor are associated with epididymosomes and spermatozoa in the bovine epididymis. Biol Reprod 2003; 69:1586–1592.
34. Frenette G, Lessard C, Sullivan R. Selected proteins of "prostasome-like particles" from epididymal cauda fluid are transferred to epididymal caput spermatozoa in bull. Biol Reprod 2002; 67:308–313.
35. Frenette G, Sullivan R. Prostasome-like particles are involved in the transfer of P25b from the bovine epididymal fluid to the sperm surface. Mol Reprod Dev 2001; 59:115–121.
36. Burg MB. Molecular basis of osmotic regulation. Am J Physiol 1995; 268: F983–F996.
37. Hoshi A, Takahashi M, Fujii J, Myint T, Kaneto H, Suzuki K, Yamasaki Y, Kamada T, Taniguchi N. Glycation and inactivation of sorbitol dehydrogenase in normal and diabetic rats. Biochem J 1996; 318(pt 1): 119–123.
38. Burant CF, Takeda J, Brot-Laroche E, Bell GI, Davidson NO. Fructose transporter in human spermatozoa and small intestine is GLUT5. J Biol Chem 1992; 267:14523–14526.
39. Glander HJ, Dettmer D. Monosaccharide transport across membranes of human spermatozoa. I. Development of a radiochemical method of

measuring monosaccharide uptake by spermatozoa. Andrologia 1978; 10: 69–73.
40. Glander HJ, Dettmer D. Monosaccharide transport across membranes of human spermatozoa. II. Basic properties of D-fructose and D-glucose uptake. Andrologia 1978; 10:273–277.
41. Qazi PH, Johri S, Verma V, Khan L, Qazi GN. Cloning, sequencing and partial characterisation of sorbitol transporter (srlT) gene encoding phosphotransferase system, glucitol/sorbitol-specific IIBC components of Erwinia herbicola ATCC 21998. Mol Biol Rep 2004; 31:143–149.
42. Grunewald RW, Ehrhard M, Fiedler GM, Schuttert JB, Oppermann M, Muller GA. Evidence for a sorbitol transport system in immortalized human renal interstitial cells. Exp Nephrol 2001; 9:405–411.
43. Kawakami E, Arai T, Nakamura U. Effects of medium containing heparin and theophylline on capacitation and metabolic enzyme activities of ejaculated spermatozoa from dogs with asthenozoospermia. Anim Reprod Sci 1999; 54:251–259.
44. Albarracin JL, Fernandez-Novell JM, Ballester J, Rauch MC, Quintero-Moreno A, Pena A, Mogas T, Rigau T, Yanez A, Guinovart JJ, Slebe JC, Concha II, Rodriguez-Gil JE. Gluconeogenesis-linked glycogen metabolism is important in the achievement of in vitro capacitation of dog spermatozoa in a medium without glucose. Biol Reprod 2004; 71:1437–1445.
45. Kamp G, Schmidt H, Stypa H, Feiden S, Mahling C, Wegener G. Regulatory properties of 6-phosphofructokinase and control of glycolysis in boar spermatozoa. Reproduction 2007; 133:29–40.
46. Burant CF, Davidson NO. GLUT3 glucose transporter isoform in rat testis: localization, effect of diabetes mellitus, and comparison to human testis. Am J Physiol 1994; 267:R1488–R1495.
47. San Agustin JT, Witman GB. Reactivation of demembranated, cytosol-free ram spermatozoa. Cell Motil Cytoskeleton 1993; 24:264–273.
48. Hagopian K, Ramsey JJ, Weindruch R. Fructose metabolizing enzymes from mouse liver: influence of age and caloric restriction. Biochim Biophys Acta 2005; 1721:37–43.
49. Holmes RS, Duley JA, Hilgers J. Sorbitol dehydrogenase genetics in the mouse: a 'null' mutant in a 'European' C57BL strain. Anim Blood Groups Biochem Genet 1982; 13:263–272.